The Plant Cell, Vol. 23: 1468–1479, April 2011, www.plantcell.org © 2011 American Society of Plant Biologists

Photoprotective Energy Dissipation Involves the Reorganization of Photosystem II Light-Harvesting Complexes in the Grana Membranes of Spinach Chloroplasts [W]

Matthew P. Johnson,[a] Tomasz K. Goral,[a] Christopher D.P. Duffy,[a] Anthony P.R. Brain,[b] Conrad W. Mullineaux,[a] and Alexander V. Ruban[a,1]

[a] School of Biological and Chemical Sciences, Queen Mary University of London, London E1 4NS, United Kingdom
[b] Centre for Ultrastructural Imaging, Kings College University of London, London SE1 1UL, United Kingdom

Plants must regulate their use of absorbed light energy on a minute-by-minute basis to maximize the efficiency of photosynthesis and to protect photosystem II (PSII) reaction centers from photooxidative damage. The regulation of light harvesting involves the photoprotective dissipation of excess absorbed light energy in the light-harvesting antenna complexes (LHCs) as heat. Here, we report an investigation into the structural basis of light-harvesting regulation in intact spinach (*Spinacia oleracea*) chloroplasts using freeze-fracture electron microscopy, combined with laser confocal microscopy employing the fluorescence recovery after photobleaching technique. The results demonstrate that formation of the photoprotective state requires a structural reorganization of the photosynthetic membrane involving dissociation of LHCII from PSII and its aggregation. The structural changes are manifested by a reduced mobility of LHC antenna chlorophyll proteins. It is demonstrated that these changes occur rapidly and reversibly within 5 min of illumination and dark relaxation, are dependent on ΔpH, and are enhanced by the deepoxidation of violaxanthin to zeaxanthin.

INTRODUCTION

Photosystem II (PSII), in the thylakoid membrane of higher plants, possesses an extensive system of membrane-associated light-harvesting antenna complexes that increase its spectral and spatial cross section of absorbed solar energy, ensuring its efficient operation, even in low light (reviewed in Dekker and Boekema, 2005). PSII is organized within the stacked grana regions of the thylakoid membranes as a dimer composed of two copies each of the reaction center core proteins D1 and D2 and the core antenna chlorophyll *a* binding proteins CP43 and CP47 (Peter and Thornber, 1991a). This PSII core dimer is further supplemented by a peripheral antenna system of chlorophyll *a/b* binding light-harvesting complexes (LHCs). The LHCs are divided into two classes: the monomeric minor antenna complexes, CP29, CP26, and CP24, and the trimeric major antenna complexes, LHCII (Peter and Thornber, 1991b). Each PSII core dimer is bound by two copies each of the minor antenna complexes CP29 and CP26 and an LHCII trimer (termed the S-trimer as the most strongly attached to the core dimer) to form the C_2S_2 supercomplex (Boekema et al., 1995). The C_2S_2 supercomplex may in turn be bound by two copies of CP24 and two LHCII trimers attached with medium strength (the M-trimers) to form the larger $C_2S_2M_2$ supercomplex (Boekema et al., 1998). These supercomplexes represent the basic functional units of the PSII-LHCII macrostructure and can be supplemented by an additional three to four loosely attached LHCII trimers (L-trimers) (Boekema et al., 1999; Dekker et al., 1999). These C_2S_2 and $C_2S_2M_2$ PSII-LHCII supercomplexes can also further become arranged into higher-order semicrystalline arrays (Miller et al., 1976; Staehelin, 1976; Boekema et al., 2000; Kirchhoff et al., 2007a; Daum et al., 2010). In contrast with PSII, photosystem I and the ATP synthase complex are mainly confined to the non-appressed stromal lamellae regions of the thylakoid membrane and the grana end membranes (reviewed in Hankamer et al., 1997; Dekker and Boekema, 2005; Daum et al., 2010).

Fluctuations in light intensity reaching the leaf, caused by the diurnal cycle and intermittent cloud cover, can limit the rate of photosynthesis in higher plants, thus creating a requirement for the dynamic regulation of light harvesting on a minute-by-minute basis. In high light, the rate of turnover of PSII reaction centers becomes saturated with respect to light; however, its absorption continues unabated. Under these conditions, the buildup of the excess excitation energy in antenna systems will inevitably lead to photoinhibition, a sustained decline in photosynthetic efficiency and productivity associated with the damage of PSII reaction centers (Powles, 1984). Fortunately, a safety valve, known as nonphotochemical quenching (NPQ), exists that is able to dissipate the excess absorbed energy as heat within the PSII antenna, preventing such photooxidative damage (reviewed in Horton et al., 1996). NPQ can be monitored by the quenching of chlorophyll fluorescence and is kinetically a heterogeneous process. The major component of NPQ is controlled by the amplitude of the transmembrane proton gradient (ΔpH) (Wraight and Crofts, 1970; Briantais et al., 1979) formed by coupled photosynthetic electron transport and is known as qE. ΔpH has several different effects upon the thylakoid membrane that act to

[1] Address correspondence to a.ruban@qmul.ac.uk.
The author responsible for distribution of materials integral to the findings presented in this article in accordance with the policy described in the Instructions for Authors (www.plantcell.org) is: Alexander V. Ruban (a.ruban@qmul.ac.uk).
[W] Online version contains Web-only data.
www.plantcell.org/cgi/doi/10.1105/tpc.110.081646

control qE. When ΔpH is high (i.e., the lumen pH is low), certain LHCs and the PsbS protein are protonated (Walters et al., 1994; Li et al., 2004) and the violaxanthin deepoxidase enzyme is activated (Hager, 1969; Demmig-Adams, 1990). Violaxanthin deepoxidase enzyme converts the xanthophyll violaxanthin, bound to peripheral sites on LHC proteins (Ruban et al., 1999; Liu et al., 2004), into zeaxanthin via the removal of two-epoxy groups (Yamamoto et al., 1962). Although the exact interplay between these three factors remains under investigation, they result in the formation of dissipative pigment interactions within one, several, or all of the LHC antenna complexe, thus shortening the chlorophyll excited state lifetime (Gilmore et al., 1995; Holzwarth et al., 2009; Johnson and Ruban, 2009). The exact pigments involved in quenching remain under debate with both chlorophyll–xanthophyll (Ma et al., 2003; Holt et al., 2005; Ruban et al., 2007; Ahn et al., 2008; Bode et al., 2009) and chlorophyll–chlorophyll interactions suggested to be involved (Müller et al., 2010). Irrespective of the pigments involved, each model assumes that a ΔpH-induced structural change activates the quenching pigment(s). However, direct structural evidence for a ΔpH-induced change in LHC antenna conformation/organization in vivo is lacking.

The first evidence that the light-driven formation of ΔpH had a structural effect on the thylakoid membrane came from work by Murakami and Packer (1970a, 1970b), who showed that it caused the thylakoid grana membranes to become thinner, more tightly appressed, and more hydrophobic. This change in properties of the thylakoid membrane was correlated with an absorption change at 535 nm (ΔA535), which was suggested to arise from selective light scattering (Murakami and Packer, 1970b). Later, ΔA535 was shown to largely depend on the presence of zeaxanthin (Bilger et al., 1989) and was correlated not to ΔpH formation per se, but rather to qE (Horton et al., 1991). Indirect evidence that qE involves a structural change within the thylakoid membrane has been provided by a range of spectroscopic methods. qE is characterized by a series of absorption and fluorescence changes (Horton et al., 1991; Ruban et al., 1991, 1992, 1993; Bilger and Björkman, 1994; Miloslavina et al., 2008; Holzwarth et al., 2009) that have been shown to depend on the composition of pigments within the LHC antenna system (Johnson and Ruban, 2009; Johnson et al., 2009). Changes in the molecular configuration and interactions between pigments upon qE formation have also been demonstrated using resonance Raman, circular dichroism, linear dichrosim, and two-photon excitation spectroscopy (Ruban et al., 1997, 2002, 2007; Bode et al., 2009; Ilioaia et al., 2011). The similarities between these qE-related spectroscopic signatures and those observed when purified LHCs adopt quenched states upon aggregation in vitro has led to the suggestion that changes in LHC conformation and/or organization underlie qE in vivo (Horton et al., 1991). The finding that aggregation induced quenching can be modulated by low pH and xanthophyll cycle carotenoids provided a further link between these phenomena (reviewed in Horton et al., 2005).

Studies on mutants lacking certain PSII antenna proteins and xanthophylls, such as zeaxanthin and lutein, have provided circumstantial evidence that changes in the PSII-LHCII macrostructure are a crucial element in the regulation of qE (reviewed in Horton et al., 2008). For instance, the *aslhcb2* and *lut2* mutants of *Arabidopsis thaliana*, which are disrupted in LHCII trimer formation and thus have a smaller PSII antenna size, showed reduced levels of qE compared with wild-type plants (Lokstein et al., 2002; Andersson et al., 2003). *Arabidopsis* plants lacking CP24 and CP29 also showed disruption in the PSII-LHCII macrostructure and somewhat reduced levels of qE compared with the wild type (Andersson et al., 2001; Kovács et al., 2006). The absence of the PsbS protein was associated with the complete absence of rapidly reversible qE-type quenching in *Arabidopsis* (Li et al., 2000), and this phenotype was accompanied by certain changes in the PSII-LHCII macrostructure (Kiss et al., 2008; Kereïche et al., 2010). More recently, in negatively stained detergent-isolated grana membranes, derived from light-treated *Arabidopsis* leaves, a PsbS-dependent change in the distance between PSII core complexes was observed by electron microscopy (EM), implying a reorganization of the PSII-LHCII macrostructure may indeed occur during illumination (Betterle et al., 2009). This was supported by biochemical evidence that showed a fragment of the $C_2S_2M_2$ supercomplex, consisting of the LHCII M-trimer, CP24, and CP29 (B4C subcomplex), is dissociated by light treatment (Betterle et al., 2009). The dissociation of the B4C subcomplex was also dependent on the presence of PsbS (Betterle et al., 2009), consistent with evidence that PsbS levels control the organization and amount of semicrystalline PSII-LHCII arrays present in *Arabidopsis* thylakoid membranes (Kiss et al., 2008; Kereïche et al., 2010).

In this work, the structural and dynamic changes that underlie the transition between the light-harvesting and photoprotective states of the thylakoid membrane were investigated using freeze-fracture EM and laser confocal microscopy on intact chloroplasts. Freeze-fracture EM has several advantages over negative stain EM in that intact chloroplasts possessing high levels of NPQ can be rapidly frozen and examined. Thus, the organization of the intact photosynthetic membrane at the level of individual PSII and LHCII complexes can be probed without the need for lengthy detergent isolation or staining procedures. The results obtained confirm findings by Betterle et al. (2009) on the light-induced alterations in the distances between PSII complexes and explicitly reveal the rapid alterations in PSII particle size, the arrangement of LHCII complexes, and the changes in protein mobility that lead to the establishment of the photoprotective state and provide further evidence that zeaxanthin has a structural role in regulating the LHCII antenna by promoting the aggregation process and, thus, quenching.

RESULTS

The Photoprotective Structural Change Remodels the PSII-LHCII Protein Landscape

We investigated whether the major rapidly reversible component of NPQ, qE, involved rapid alterations in the macroorganization of PSII-LHCII using freeze-fracture EM. Spinach (*Spinacia oleracea*) chloroplasts were harvested from either dark-adapted leaves (Vio) or leaves preilluminated to accumulate zeaxanthin (Zea) (Table 1). Chlorophyll fluorescence quenching kinetics of the two types of chloroplasts are shown in Figure 1. By dividing the quenched fluorescence by the unquenched fluorescence,

Table 1. Pigment Composition and NPQ Values for Intact Spinach Chloroplasts

Sample	Neo	Lut	XC	DEPs%	Chlorophyll *a*/*b*	NPQ
Dark Vio	45 ± 2.8	122 ± 3	50 ± 2.8	0	3.5 ± 0.1	0
Light Vio	44 ± 1.6	122 ± 2	49 ± 1.1	0	3.4 ± 0.09	0.6 ± 0.1*
Light Zea	45 ± 1.1	121 ± 2	49 ± 1.3	35 ± 1.3*	3.5 ± 0.1	2.1 ± 0.1*
Dark Zea	46 ± 0.8	120 ± 3	49 ± 2.1	36 ± 3.7*	3.5 ± 0.07	0.3 ± 0.03*
Light nigericin	44 ± 2.4	121 ± 3	50 ± 2.3	0	3.4 ± 0.1	0

Chloroplasts devoid of zeaxanthin and antheraxanthin (Vio) and chloroplasts enriched in zeaxanthin (Zea) were light treated for 5 min at 350 μmol photons m^{-2} s^{-1} to form NPQ and then either immediately frozen for pigment analysis (*Light Vio* and *Light Zea* chloroplasts) or given a further 5 min of darkness to allow NPQ to relax prior to freezing for pigment analysis. A separate sample of Vio chloroplasts was light treated at 350 μmol photons m^{-2} s^{-1} for 5 min in the presence of 2 μM nigericin (*Light nigericin*). Data are expressed as mmoles carotenoids per mole chlorophyll *a* + *b* molecules and are means ± SE from four replicates. Neo, Lut, XC, DEPs, and chlorophyll *a*/*b*, NPQ correspond to neoxanthin, lutein, xanthophyll cycle carotenoids (violaxanthin, antheraxanthin, and zeaxanthin), xanthophyll cycle deepoxidation state [(Z+0.5A)/(V+A+Z)]%, chlorophyll *a*/*b* ratio, and the amount of NPQ in each sample as calculated from chlorophyll fluorescence traces as shown in Figure 1. For the statistical confidence levels, the asterisk indicates a significant difference with respect to dark-adapted sample ($P < 0.01$, using analysis of variance, Tukey contrast).

the amplitude of NPQ was calculated for each type of chloroplast. For Zea chloroplasts, an NPQ amplitude of 2.1 ± 0.1 was obtained following 5 min illumination, while in Vio chloroplasts, the NPQ amplitude was 0.6 ± 0.1 (Table 1). The level of 9-aminoacridine quenching confirmed that the amplitude of ΔpH was the same in each type of chloroplast (see Supplemental Figure 1 online). Samples of chloroplasts were either taken immediately after 5 min of illumination or following a further 5-min period of darkness to allow relaxation of the qE component of NPQ (Figure 1, Table 1). Four samples of chloroplasts were thus obtained for freeze-fracture analysis, hereafter referred to as *Dark Vio*, *Light Vio*, *Dark Zea*, and *Light Zea*, as labeled in Figure 1. The freeze-fracture technique splits hydrophobic core of the membrane bilayer into the exoplasmic and protoplasmic leaflets, allowing information on the organization and dimensions of the proteins therein to be determined by image analysis. Four distinct fracture faces are observed in freeze-fracture EM images (reviewed in Staehelin, 2003) (Figure 2A). The exoplasmic fracture face of the stacked membranes (EFs) is dominated by PSII particles of ~16 to 18 nm (Staehelin, 1976; Armond et al., 1977). The complementary protoplasmic fracture face of the stacked membranes (PFs) contains the ~8-nm LHCII particles (Miller et al., 1976; Simpson, 1979). The protoplasmic fracture face of the unstacked membranes is distinguished on the basis of its slightly larger asymmetric ~10-nm photosystem I particles (Simpson, 1982). Finally, the complementary exoplasmic fracture face of the unstacked membranes is largely smooth and marked by generally more widely spaced ~10- to 16-nm PSII particles (Staehelin, 1976; Armond et al., 1977). In the *Dark Vio* chloroplasts, the PSII particles on the EFs fracture faces were generally well spaced (Figure 2A). In the *Light Vio* chloroplasts, there was a noticeable tendency for the PSII particles on the EFs fracture faces to become more tightly clustered together (Figure 2B). The clustering of the PSII particles appeared even more pronounced in the *Light Zea* chloroplasts (Figure 2C, arrow 1), while in the *Dark Zea* chloroplasts, the EFs fracture faces appeared similar to those in the *Light Vio* chloroplasts (Figure 2D). Image analysis allowed the changes in PSII clustering, nearest-neighbor distance, and particle size in each type of chloroplast to be quantified (see Supplemental Figure 2 online). The clustering of PSII particles was quantified by calculating the number of EFs particles within a 50-nm radius of any given EFs particle, with normalization to account for variation in the area of EFs fracture faces from one image to another. The normalization was necessary to remove edge effects or the tendency for particles at the edge of a fracture face to have fewer neighbors than those nearer to the center. The PSII clustering was significantly increased in the *Light Vio* chloroplasts relative to the *Dark Vio* chloroplasts, and these changes were further enhanced in the *Light Zea* chloroplasts (Figure 3A, Table 2). The change in PSII clustering was partially reversed in the *Dark Zea* chloroplasts compared with the *Light Zea* chloroplasts, with distribution similar to that found in the *Light Vio* chloroplasts (Figure 3A, Table 2). A similar pattern was observed using the nearest-neighbor

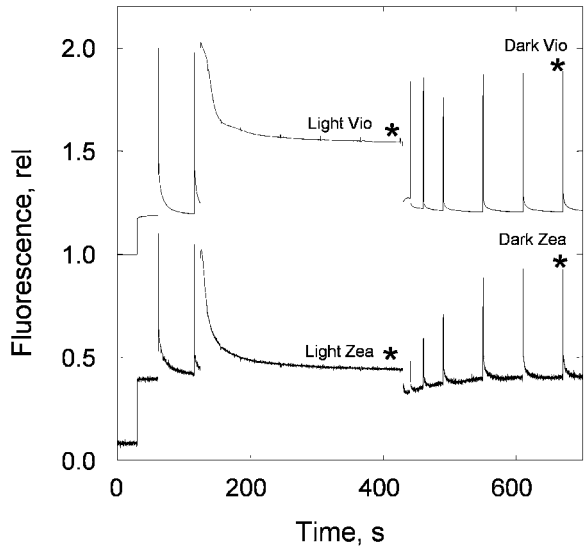

Figure 1. Chlorophyll Fluorescence Quenching Kinetics of Intact Spinach Chloroplasts Treated for 5 min with 350 μmol photons m^{-2} s^{-1} light.

Zea chloroplasts contain zeaxanthin, while Vio chloroplasts are devoid of zeaxanthin (see Table 1). After 5 min of light treatment, the chloroplasts were frozen (for freeze-fracture EM) immediately (**Light Vio* and *Light Zea* samples) or allowed a further 5 min of darkness to relax NPQ prior to freezing (**Dark Vio* and *Dark Zea* samples).

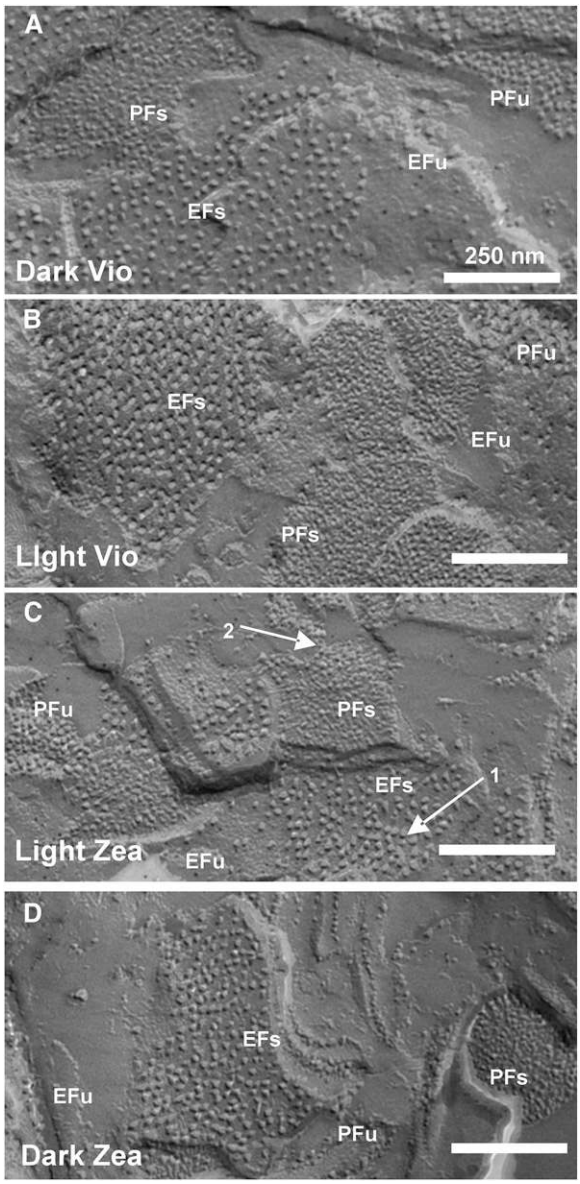

Figure 2. Freeze-Fracture Electron Microscopy of Intact Chloroplasts.

Freeze-fracture electron micrographs showing the thylakoid membrane structure in *Dark Vio* **(A)**, *Light Vio* **(B)**, *Light Zea* **(C)** [inset arrows highlight areas with enhanced clustering of PSII (1) and LHCII (2)], and *Dark Zea* **(D)** intact spinach chloroplasts prepared as shown in Figure 1. EFs and PFs, exoplasmic and periplasmic fracture faces of the stacked grana regions of the thylakoid membrane; EFu and PFu, exoplasmic and periplasmic fracture faces of stromal lamellae regions of the thylakoid membrane.

distance between PSII particles as a measure of their association (Kirchhoff et al., 2007b; Betterle et al., 2009) (Figure 3B, Table 2), confirming the increased tendency of PSII to cluster in the *Light Zea* sample. If 2 μM of the uncoupler nigericin was added to chloroplasts just prior to 5 min of illumination, hereafter referred to as *Light nigericin* (Table 1), no change in PSII particle size, PSII clustering, or PSII nearest-neighbor distances was observed (Table 2). The changes in PSII-LHCII macrostructure seen in the light therefore depend on the formation of ΔpH.

The other noticeable tendency in the *Light Zea* chloroplasts was the smaller size of the PSII particle compared with the *Dark Vio* sample, with the PSII particles in the *Light Vio* and *Dark Zea* samples appearing somewhat intermediate in terms of size (Figures 4A to 4D). Using image analysis, these differences could be quantified allowing the distribution of PSII particle sizes to be plotted for each type of chloroplast (Figure 4E, Table 2). The analysis of PSII particle size demonstrated that the average decreased from ~200 nm^2 in the *Dark Vio* chloroplasts to ~125 nm^2 in the *Light Zea* chloroplasts, with an increase in the population of particles in the 100- to 150-nm^2 range at the expense of those above 200 nm^2 (Figure 4E, Table 2). The average size of the EFs fracture face PSII particles in the dark is too large to simply represent a PSII core dimer (145 nm^2) (Hankamer et al., 1997),

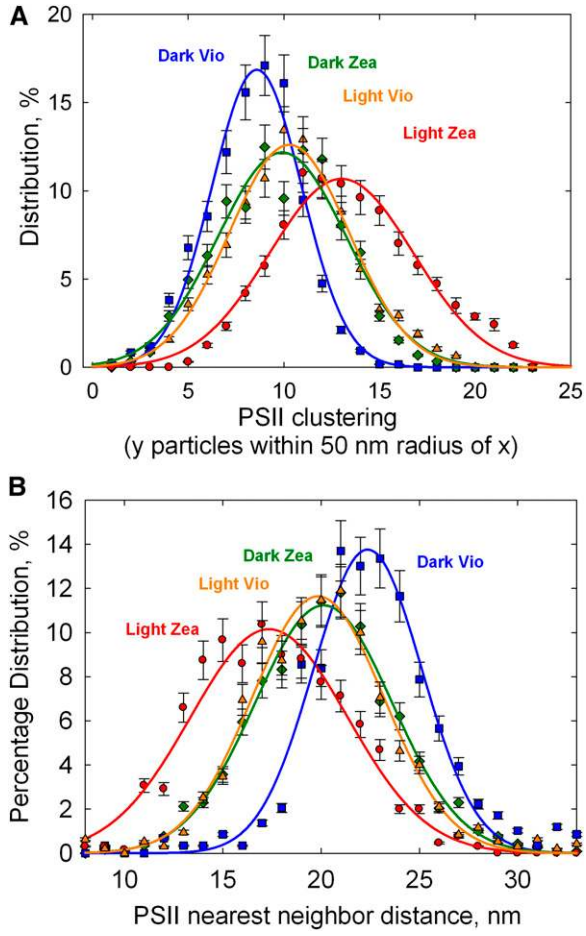

Figure 3. Analysis of PSII EFs Fracture Faces from Freeze-Fracture Electron Micrographs of Intact Spinach Chloroplasts.

Graphs showing the percentage distribution of PSII clustering **(A)** (number of neighboring PSII particles within a 50-nm radius of a given PSII particle) and PSII nearest-neighbor (center-to-center) distance **(B)**. Data are averaged from three independent experiments (±SE%). See Table 2 for statistics.

Table 2. Analysis of EFs and PFs Fracture Faces from Electron Micrographs of Intact Spinach Chloroplasts

Sample	No. of PSII Particles Analyzed	PSII Nearest-Neighbor Distance (nm)	PSII Clustering, No. of Particles within 50 nm of x	PSII Particle Size (nm^2)	No. of LHCII Particles Analyzed	LHCII Clustering, No. of Particles within 25 nm of x	LHCII Particle Size (nm^2)
Dark Vio	2610	24.3 ± 2	8.6 ± 0.5	198 ± 12	6304	7.7 ± 0.5	50 ± 3
Light Vio	2712	20.4 ± 3*	9.9 ± 0.4*	148 ± 13*	5760	10.6 ± 0.5*	54 ± 5
Dark Zea	2561	20.9 ± 2*	10.3 ± 0.5*	157 ± 12*	6689	11.5 ± 0.5*	48 ± 5
Light Zea	2208	17.3 ± 2**	13.0 ± 0.5**	126 ± 8*	6334	16.9 ± 0.5**	55 ± 5
Light nigericin	1312	24.5 ± 3	8.2 ± 0.7	201 ± 15	3120	7.5 ± 0.8	52 ± 3

Chloroplasts devoid of zeaxanthin and antheraxanthin (Vio) and chloroplasts enriched in zeaxanthin (Zea) were light treated for 5 min at 350 μmol photons m^{-2} s^{-1} to form NPQ and then either immediately frozen for freeze-fracture EM analysis (*Light Vio* and *Light Zea* chloroplasts) or given a further 5 min of darkness to allow NPQ to relax prior to freezing for freeze-fracture EM analysis (*Dark Vio* and *Dark Zea* chloroplasts). A separate sample of Vio chloroplasts was light treated at 350 μmol photons m^{-2} s^{-1} for 5 min in the presence of 2 μM nigericin (*Light nigericin*). For the statistical confidence levels, the asterisk indicates a significant difference with respect to dark-adapted sample ($P < 0.01$, using analysis of variance, Tukey contrast).

but most of the observed particles are too small to represent a C_2S_2-type PSII supercomplex (310 nm^2) (Boekema et al., 1995). Rather, the size of the PSII particles is most consistent with a PSII core dimer and two to three minor antenna proteins (~220 nm^2) (Boekema et al., 1995). This conclusion is consistent with the fact that *Arabidopsis* mutants lacking certain minor antenna complexes, the most closely bound LHCs to the PSII core (Boekema et al., 1995), contained smaller PSII particles than the wild type (see Supplemental Table 1 online) and with previous observations suggesting a part of the attached LHC complexes may also fracture with the EFs face under certain conditions (Armond et al., 1977). Thus, NPQ is associated not only with a clustering of PSII particles on the EFs fracture faces but also a reduction in their apparent size.

The PFs fracture face containing LHCII particles is complementary to the EFs PSII fracture face (Simpson, 1979; Staehelin, 2003). There was a noticeable increase in the packing of LHCII complexes on the PFs fracture faces in the *Light Zea* chloroplasts (Figure 3C, arrow 2) compared with the *Dark Vio* chloroplasts (Figure 3A). Higher-magnification images of PFs fracture faces from *Dark Vio* and *Light Zea* chloroplasts are shown in Figures 5A and 5B. In the *Dark Vio* chloroplasts, the LHCII particles are fairly evenly distributed across the fracture face with clear gaps among the LHCII particles (Figure 5A, arrows) that are likely to correspond to space occupied in the membrane by the PSII particles that fracture with the EFs face. By contrast, in the *Light Zea* chloroplasts, the PFs fracture faces are marked by areas of very high LHCII particle density, where very few gaps are visible (Figure 5B, arrow 1), and areas of much lower density, where LHCII particles are more sparse (Figure 5B, arrow 2), likely corresponding to areas of PSII clustering on the opposing EFs fracture face. The increased clustering of LHCII can be quantified from the number of neighboring LHCII particles within a 25-nm radius of a given LHCII particle (see Supplemental Figure 2 online). The analysis confirmed the increase in clustering in the *Light Zea* chloroplasts relative to the *Dark Vio* chloroplasts (Figure 5C). In the *Light Vio* chloroplasts, the changes in LHCII clustering were smaller than in the *Light Zea* chloroplasts (Figure 5C, Table 2), while the changes in the *Light Zea* chloroplasts were partially reversed in the *Dark Zea* sample (Figure 5C, Table 2). Thus, zeaxanthin is associated with an enhancement of both the clustering of LHCII and PSII particles observed in chloroplasts exhibiting the NPQ state. The relative size of the LHCII particles was ~50 nm^2, which is consistent with the size of an LHCII trimer (Dekker and Boekema, 2005) (Figure 5D, Table 2). Unlike for the PSII particles on the EFs fracture faces, the size of the LHCII particles on the PFs fracture faces was observed to be fairly constant in all four chloroplast samples (Figure 5D, Table 2), suggesting the LHCII trimer remains intact. The changes in LHCII clustering were also found to be dependent upon the formation of ΔpH since they were absent in *Light nigericin* chloroplasts (Table 2).

The Mobility of Chlorophyll Proteins Is Reduced in the Photoprotective State

Using confocal laser microscopy, it was possible to image the intact chloroplasts prepared as in Figure 1 (Figure 6A). The autofluorescence of the chlorophyll within the thylakoid membranes can be visualized within the chloroplasts, with grana appearing as brighter spots (Goral et al., 2010) (Figure 6A). The intact chloroplasts could be distinguished from those that were broken by the use of the lipid staining green fluorescent dye (BODIPY FL C_{12}), which is bound by the outer envelope membrane only, while in broken chloroplasts the dye can also stain the thylakoid membrane (Figure 6A). The fluorescence recovery after photobleaching (FRAP) technique involves the bleaching of a selected region of fluorescence from the thylakoid membrane within an intact chloroplast using a strong laser pulse (Kirchhoff et al., 2008; Goral et al., 2010) (Figure 6A). The kinetics of fluorescence recovery in the bleached region can then be recorded to allow calculation of the mobile fraction of chlorophyll-proteins within the thylakoid membrane (Kirchhoff et al., 2008; Goral et al., 2010) (Figure 6B). The mobile fraction has proved to be a useful and reproducible indicator of protein mobility in chloroplasts (Goral et al., 2010). The recovery of the chlorophyll fluorescence in the bleached region of the *Dark Vio* chloroplasts used in this study was ~12 to 15%, while the recovery of the lipid dye fluorescence in the thylakoid membrane (as determined from broken chloroplasts) was ~100% (Figure 6B). Thus, the thylakoid membrane remains intact after bleach, with the lower mobility of the chlorophyll binding proteins

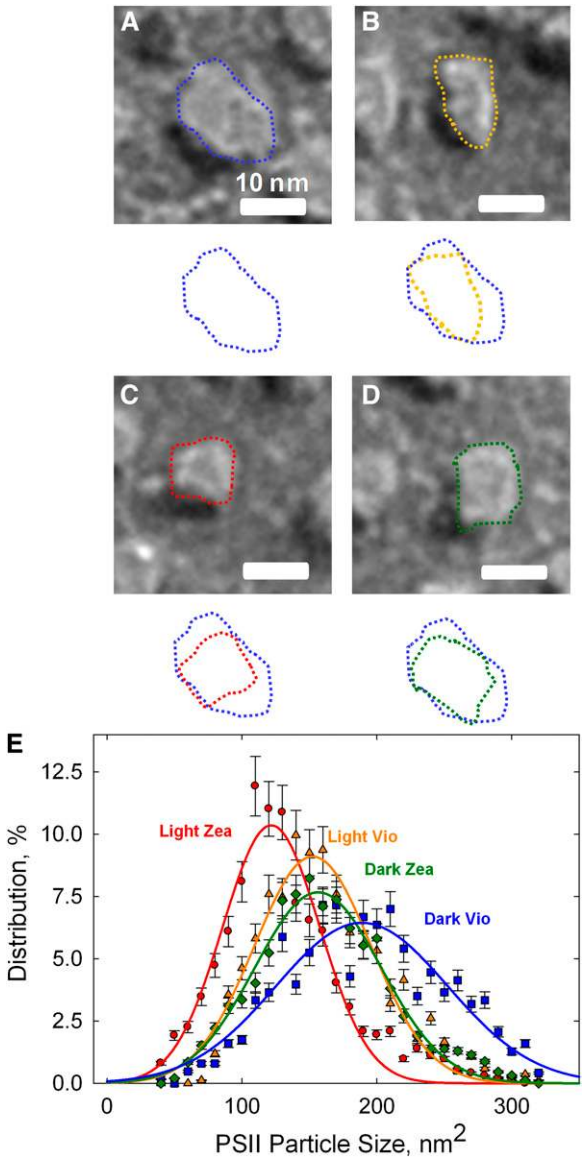

Figure 4. Freeze-Fracture Electron Microscopy of PSII in the Thylakoid Membrane.

(A) to **(D)** Representative freeze-fracture electron micrographs showing EFs PSII particles from each type of chloroplast, with an outline of the area of each particle compared with the *Dark Vio* particle **(A)** (blue outline) shown below. *Light Vio* PSII particle **(B)** (orange outline), *Light Zea* PSII particle **(C)** (red outline), and *Dark Zea* PSII particle **(D)** (green outline).
(E) Graph showing percentage distribution of PSII particle size (area) in *Dark Vio* (blue squares), *Light Vio* (orange triangles), *Light Zea* (red circles), and *Dark Zea* (green diamonds) intact spinach chloroplasts. Data are averaged from three independent experiments (±SE%). See Table 2 for statistics.

compared with the lipids likely reflecting the extremely crowded protein environment in vivo (Kirchhoff et al., 2008; Goral et al., 2010). The observed reorganization of the PSII and LHCII particles in the NPQ state was characterized by a 35% reduction in chlorophyll-protein mobility in the *Light Zea* chloroplasts compared with the *Dark Vio* chloroplasts (Figure 6C). Consistent with the lower amount of NPQ in *Light Vio* and *Dark Zea* chloroplasts, the reduction in the size of the mobile fraction of chlorophyll-proteins was less than in the *Light Zea* sample (Figure 6C).

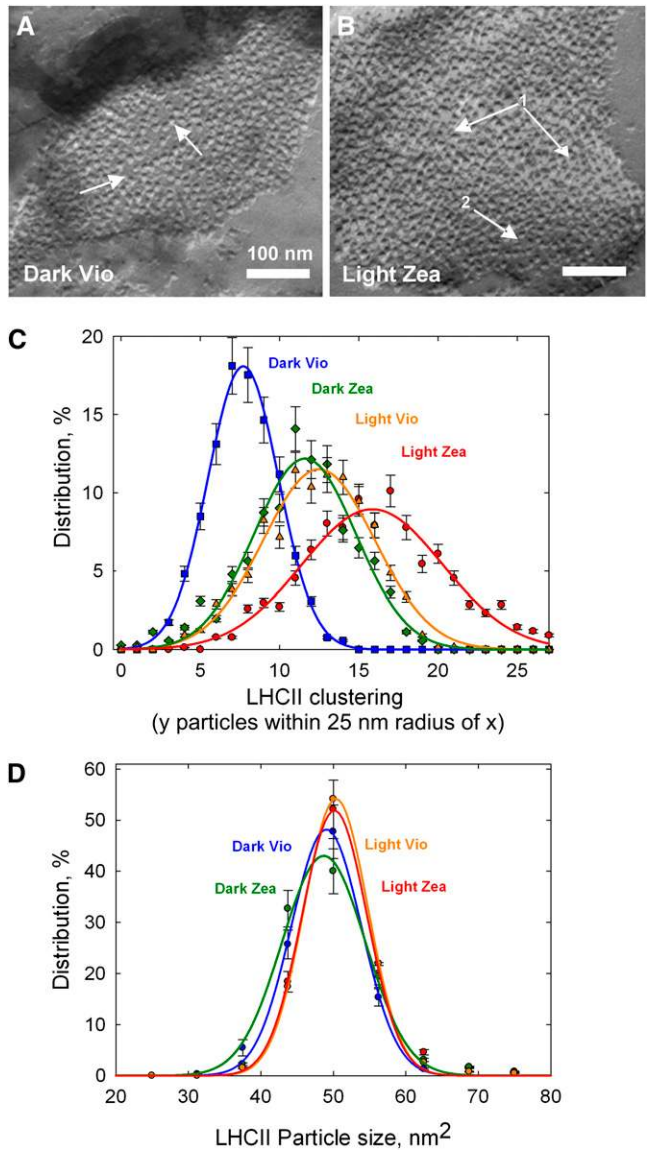

Figure 5. Freeze-Fracture Electron Microscopy of LHCII in the Thylakoid Membrane.

Higher-magnification view of LHCII PFs fracture faces in freeze-fracture electron micrographs of *Dark Vio* **(A)** and *Light Zea* **(B)** intact spinach chloroplasts [inset arrows highlight areas with enhanced (1) and reduced (2) clustering of LHCII] prepared as shown in Figure 1. Analysis of LHCII PFs fracture faces from freeze-fracture electron micrographs of intact spinach chloroplasts. Graphs showing the percentage distribution of LHCII clustering **(C)** (number of neighboring LHCII particles within a 25-nm radius of a given LHCII particle) and LHCII particle size **(D)** (area) in *Dark Vio* (blue squares), *Light Vio* (orange triangles), *Light Zea* (red circles), and *Dark Zea* (green diamonds) intact spinach chloroplasts. Data are averaged from three independent experiments (±SE%). See Table 2 for statistics.

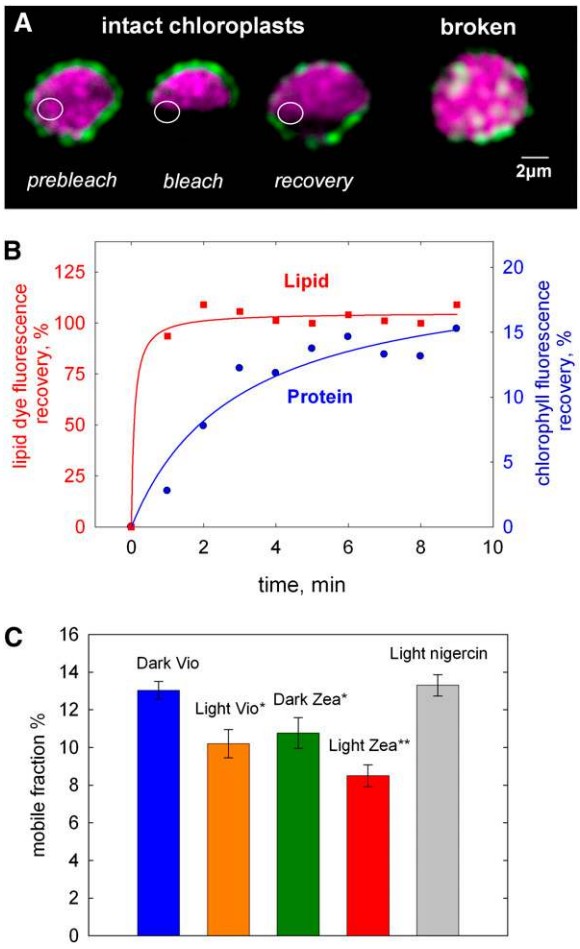

Figure 6. Fluorescence Recovery after Photobleaching Study of Intact Chloroplast Membranes.

(A) Typical laser confocal microscopy images on intact (left) and broken (far right) chloroplasts. The white circles highlight a grana membrane within the thylakoid that is bleached by the laser during the FRAP experiment and then monitored for fluorescence recovery, with BODIPY fluorescence shown in green and chlorophyll fluorescence in magenta.
(B) Kinetics of BODIPY (lipid), determined for broken chloroplasts, and chlorophyll (protein), determined for intact chloroplasts, fluorescence recovery in thylakoid membranes following bleaching by FRAP.
(C) Size of the mobile fraction in *Dark Vio* (blue), *Light Vio* (orange), *Dark Zea* (green), and *Light Zea* (red) intact spinach chloroplasts prepared as shown in Figure 1 (n = 10 experiments ± SE). Single asterisk indicates significant difference from *Dark Vio* sample; double asterisk indicates significant difference from *Dark Vio*, *Dark Zea*, and *Light Vio* samples (analysis of variance, Tukey contrast, 99% confidence).

DISCUSSION

qE Involves the Reorganization of PSII and LHCII within the Thylakoid Membrane

In this investigation, direct structural evidence has been provided that changes in the ultrastructure of the thylakoid membrane and in the organization of PSII and LHCII complexes within it are associated with NPQ formation. In contrast with the study of Betterle et al. (2009), where the observed changes in PSII organization took ~30 to 60 min to form and relax, the changes identified here are shown to occur within 5 min of illumination and dark relaxation consistent with their involvement in rapidly reversible qE-type quenching. We extend the findings of Betterle et al. (2009) by showing that formation of NPQ is specifically accompanied by an aggregation of major trimeric LHCII complexes, explaining the often-reported spectroscopic link between NPQ in vivo and LHCII aggregation in vitro (Horton et al., 1991; Ruban et al., 1992, 1997, 2007; Miloslavina et al., 2008; Holzwarth et al., 2009; Johnson and Ruban 2009; Liao et al., 2010). We also provide in vivo structural evidence showing that the EFs PSII particle, and by inference the PSII-LHCII supercomplex, is reduced in size during NPQ, probably due to dissociation of part of the minor light-harvesting antenna. Moreover, the changes in PSII and LHCII clustering can be correlated with NPQ and are thus influenced by the deepoxidation state of the xanthophyll cycle carotenoids (Figure 7A). We further show that formation of the photoprotective state modulates the mobility of chlorophyll-proteins within the thylakoid membrane system. When the photoprotective state is formed, the mobile population of complexes decreases, most likely due to aggregation of LHCII, providing further evidence that the packing of the complexes in the membrane influences their mobility and function (Kirchhoff et al., 2008; Goral et al., 2010) (Figure 7B). Recently, in photoinhibited spinach chloroplasts, an increase in the size of the mobile fraction of chlorophyll-proteins was observed relative to the control sample (Goral et al., 2010). The photoinhibition-related increase in the mobile fraction was shown to be dependent upon the activity of the *stn8* kinase (Goral et al., 2010), which is known to phosphorylate the PSII core complex, mediating its migration to the stromal lamellae during the PSII repair cycle (Bonardi et al., 2005). The change in the size of the mobile fraction was also correlated with decreased clustering of PSII particles in freeze-fracture electron micrographs of photoinhibited chloroplasts, relative to those of the control (Goral et al., 2010). Photoinhibition and NPQ therefore appear to have opposing effects with regards to both PSII clustering and chlorophyll-protein mobility.

We suggest that the rapid changes in the organization of PSII and LHCII complexes in the thylakoid membrane are linked to the ΔpH-induced changes in membrane thickness described by Murakami and Packer (1970a, 1970b). Previously, it has been demonstrated using linear dichroism spectroscopy that upon qE formation in vivo and upon LHCII aggregation in vitro that the xanthophylls adopt a more parallel orientation with respect to the plane of the membrane (Ruban et al., 1997). This condensed state of LHCII formed upon its aggregation may thus be the origin of the reduction in membrane thickness and increase in membrane hydrophobicity associated with qE that was discovered in the studies of Murakami and Packer (1970a, 1970b).

A Working Model for the qE-Related Structural Change

The information revealed by this study and the work of Betterle et al. (2009) on the structural basis of qE formation in vivo allows us to produce the next step in a working model first presented by

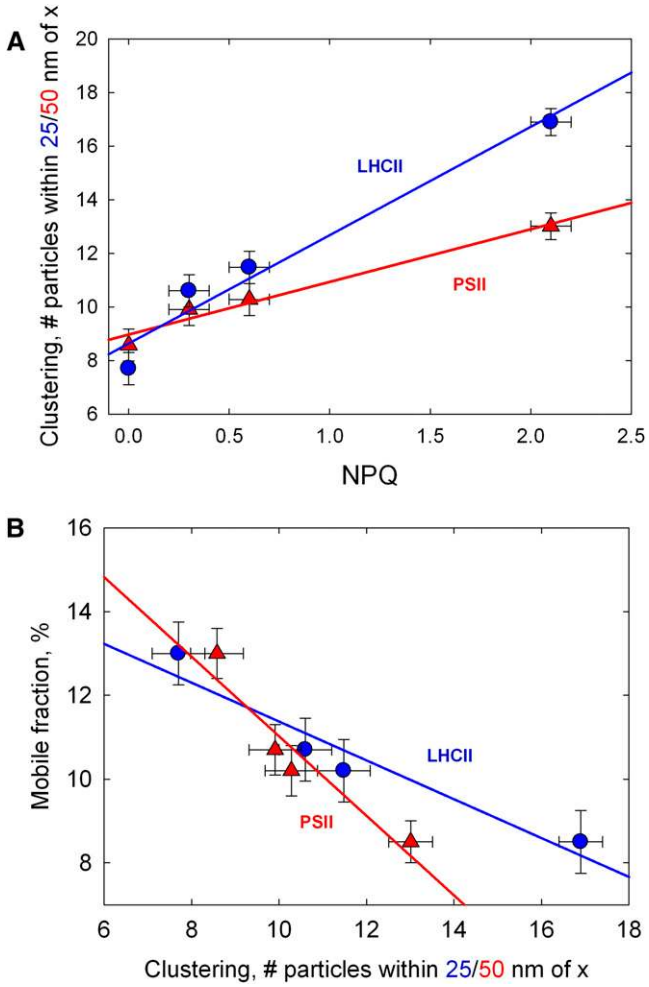

Figure 7. Protein Clustering and Mobility in PSII Membranes in the NPQ State.

Relationships between PSII (red triangles) and LHCII (blue circles) particle clustering in freeze-fracture electron micrographs and NPQ **(A)** or the mobile fraction of chlorophyll-proteins in intact spinach chloroplasts **(B)**. Data are averaged from three independent experiments (±SE%).

Horton et al. (2008), describing the structural changes (Figure 8). The left of Figure 8 depicts the lateral organization of the PSII-LHCII supercomplexes within the grana thylakoid membranes in the dark and in low light. Most of the PSII and LHCII units are organized into $C_2S_2M_2$ supercomplexes (Dekker and Boekema, 2005). Additional LHCII trimers (L-trimers) are dispersed among the $C_2S_2M_2$ supercomplexes. We suggest that ΔpH formation in excess light triggers a conformational change in LHC complexes, causing their dissociation from PSII and their aggregation (Figure 8). The partial dissociation of the PSII-LHCII supercomplex in excess light is manifested in the reduced size of the PSII EFs particle observed in our freeze-fracture electron micrographs. While we cannot be sure of exactly which of the minor antenna components is dissociated from the EFs PSII particle and which remains attached, we suggest the most likely to be detached is CP24. CP24 is the most loosely bound component of the supercomplex (Dekker and Boekema, 2005), and its dissociation would explain the reduced levels of the B4C subcomplex observed in excess light (Betterle et al., 2009). The stimulatory effect of zeaxanthin on the structural changes observed in chloroplasts may be explained by the observation that hydrophobic zeaxanthin promotes LHC aggregation and quenching in vitro by shifting the lumen pH dependence to more alkaline values (Ruban et al., 1997; Ruban and Horton, 1999). Therefore, compared with chloroplasts devoid of zeaxanthin, proton binding and, thus, the structural changes within chloroplasts are enhanced. We suggest that the conformational state of LHC proteins induced by protonation is the primary structural factor underlying the formation of internal dissipative pigment interactions, which may in principle be explained by any of the current xanthophyll-chlorophyll or chlorophyll-chlorophyll quenching models (Ruban et al., 2007; Ahn et al., 2008; Liao et al., 2010; Müller et al., 2010). In the absence of PsbS, we suggest that the more rigid PSII-LHCII macrostructure (Kereïche et al., 2010) somehow precludes these ΔpH-induced structural changes.

Conclusions

The data presented in this study provide direct structural evidence that a reorganization of PSII-LHCII supercomplexes can occur on a timescale consistent with formation and relaxation of qE. The data further define the fate of the LHCII that is excluded from the more tightly clustered areas of PSII particles first described by Betterle et al. (2009), showing that they form large clusters or aggregates within the membrane. The clustering of LHCII particles can explain the reduced mobility of chlorophyll

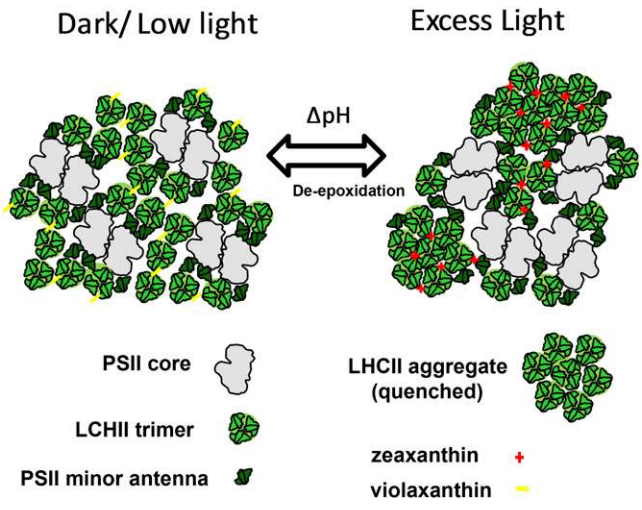

Figure 8. Structural Model of NPQ-Related Reorganization of Thylakoid Grana Membranes.

In the dark and low light, LHCII is distributed fairly evenly distributed in the grana, forming large $C_2S_2M_2$ supercomplexes with PSII and minor antenna proteins. In excess light, ΔpH triggers a conformational change within LHC complexes that causes the partial dissociation of the PSII-LHCII supercomplex and leads to LHCII aggregation. Deepoxidation of violaxanthin to zeaxanthin promotes LHCII aggregation and ,thus, NPQ.

proteins observed in the qE state by FRAP and the consistently observed spectroscopic link between qE and aggregation of LHCII in vitro. It is interesting to note that both state transitions, a mechanism of low-light adaptation, were also shown to involve the formation of LHCII aggregates in the green algae *Chlamydomonas reinhardtii* (Iwai et al., 2010). LHCII aggregation may thus be a general response of the thylakoid membrane to any unfavorable light conditions. The data therefore provide the beginnings of a macroscopic understanding of the structural changes involved in qE formation. The next step will be to understand the exact role of PsbS reorganization and the precise nature of the microscopic structural changes within LHC complexes that underlie the macroscopic change.

METHODS

Plants and Growth Conditions

Spinach (*Spinacea oleracea*) plants were grown for 6 to 7 weeks in a glasshouse under natural light conditions of an English summer.

Chloroplast Isolation

Chloroplasts devoid of zeaxanthin and antheraxanthin (Vio chloroplasts) were prepared from spinach leaves dark adapted for 1 h as previously described (Crouchman et al., 2006). Chloroplasts enriched in zeaxanthin (Zea chloroplasts) were prepared from spinach leaves light treated for 15 min at 350 μmol photons m^{-2} s^{-1} under 98% N_2/2% O_2. Chlorophyll concentration was determined as previously described (Porra et al., 1989).

Chlorophyll Fluorescence Induction and Sample Conditioning

Chlorophyll fluorescence was measured with a Dual-PAM-100 chlorophyll fluorescence photosynthesis analyzer (Heinz Walz) using the liquid cell adapter. Intact chloroplasts (1.4 mL) were measured in a quartz cuvette at a concentration of 36 μM chlorophyll under continuous stirring. The reaction medium contained 0.45 M sorbitol, 20 mM Tricine-KOH, pH 8.0, 10 mM EDTA, 10 mM $NaHCO_3$, 0.1% BSA, and 5 mM $MgCl_2$. Ascorbate was omitted from all buffers to prevent further deepoxidation taking place during illumination. 50 μM methyl viologen was provided as the terminal electron acceptor. After 5-min light treatment, the chloroplasts were frozen immediately (for freeze-fracture EM) or allowed a further 5 min of darkness to relax NPQ prior to freezing. Actinic illumination (350 μmol photons m^{-2} s^{-1}) was provided by arrays of 635-nm LEDs. F_o (the fluorescence level with PSII reaction centers open) was measured in the presence of a 10 μmol photons m^{-2} s^{-1} measuring beam. The maximum fluorescence in the dark-adapted state (F_m), during the course of actinic illumination (F_m'), and in the subsequent dark relaxation periods (F_m'') was determined using a 0.8-s saturating light pulse (4000 μmol photons m^{-2} s^{-1}). NPQ was calculated as follows $NPQ = (F_m - F_m')/F_m'$.

Measurement of ΔpH Kinetics

ΔpH was determined from the measurement of 9-aminoacridine fluorescence using a Jobin Yvon FluoroMax-3 spectrophotometer. Intact chloroplasts were treated as described above in the presence of 1 μM 9-aminoacridine. Excitation was defined at 400 nm with a 2-nm spectral bandwidth, and fluorescence emission was filtered using a Corning 4-96 filter and an OCLI Cyan T400-570 mirror and detected at 456 nm with a 5-nm slit width. The intensity of the 635-nm LED light used to induce ΔpH was 350 μmol photons m^{-2} s^{-1}. The fluorescence kinetic integration time was 0.5 s.

Pigment Analysis

Pigments were extracted from intact chloroplasts using 100% acetone. Pigment composition was determined by reversed phase HPLC using a LiChrospher 100 RP-18 column (Merck) and a Dionex Summit chromatography system as previously described (Johnson et al., 2007).

Freeze-Fracture EM

Chloroplasts were rapidly frozen in slushy liquid nitrogen and fractured at −150°C in a Polaron E7500 freeze-fracture device. Replicas were prepared by shadowing with platinum and carbon and cleaned with bleach. Freeze-fracture replicas were examined with a Hitachi H7600 or FEI Tecnai 12 BioTWIN electron microscope at a range of magnifications.

EM Image Analysis

The coordinates and dimensions of particles on the EFs and PFs faces of freeze-fracture EM images were identified with particle picker routines using ImagePro Plus software (Media Cybernetics). Nearest-neighbor distances and particle clustering were calculated from the coordinates of each particle using a bespoke program (available on request). Nearest-neighbor distance analysis of freeze-fracture EM images allows us to measure the distances with ~0.72 nm accuracy, which is the spatial resolution (single pixel size in xy direction) of our electron micrographs. If there is a change in the distance between two particles, the program would only detect the difference at the level of at least one single pixel size.

Sample Preparation for FRAP

Prior to experiments, intact chloroplast suspensions prepared in a range of states (see sample conditioning) were diluted down in the resuspension buffer containing 5 μM 4,4-difluoro-5,7-dimethyl-4-bora-3a,4a-diaza-s-indacene-3-dodecanoic acid (BODIPY FL C12; Invitrogen, Molecular Probes) to a final chlorophyll concentration of 10 μg mL^{-1}. A glass slide was sealed with a cover slip using a small amount of vacuum grease so as to form a flow chamber. Sixty microliters of a 0.5% aqueous solution of polylysine (Sigma-Aldrich) was applied to the chamber and washed with the resuspension buffer, followed by application of 60 μL of the chloroplast suspension. After 5 min incubation, the intact chloroplasts that were not immobilized were washed out with the resuspension buffer and the sample was used for FRAP measurements.

FRAP Measurements

Chlorophyll FRAP measurements were performed on intact chloroplasts with a Nikon PCM2000 confocal laser scanning microscope. The 488-nm line of a 100-mW argon laser (Spectra-Physics) was used for exciting both chlorophyll and BODIPY fluorescence. BODIPY fluorescence was selected with a 505-nm dichroic mirror and an interference filter with a transmission range of 500 to 527 nm. Chlorophyll fluorescence was selected with a Schott RG665 red-glass filter transmitting above ~665 nm. Chloroplasts were visualized with the use of a 20-μm confocal pinhole giving a point-spread in the Z-direction of ~1.3 μm (full width at half maximum). For FRAP, a line was bleached across the sample by withdrawing neutral density filters to increase laser power by a factor of 32. The laser was then scanned repeatedly in one dimension for 5 to 7 s. Laser power was then reduced again and a series of 10 postbleach images was recorded at 60-s intervals.

Image Processing and Data Analysis of FRAP Images

Laser confocal images of intact chloroplasts were converted to grey scale and deconvolved using the DeconvolutionJ plugin of the public domain

NIH ImageJ software (http://rsb.info.nih.gov/ij/). The point-spread function was determined by confocal visualization of 0.175-μm fluorescence microspheres (PS-Speck microscope point source kit; Invitrogen, Molecular Probes) with the same microscope setup. The images were then aligned with ImagePro Plus software (Media Cybernetics) and analyzed with ImageJ. An individual granum within an intact chloroplast was selected as a region of interest, and the fluorescence intensity of that region was measured in pre- and postbleach images. Simultaneously, the fluorescence in unbleached regions in postbleach images was normalized to the same total fluorescence as in prebleach images. Mobile fractions were determined by fluorescence recovery curves as presented in Figure 6B according to the following equation: $R = (F\infty - F0)/(Fi - F0)$, where R is mobile fraction, $F\infty$ is the fluorescence intensity in the bleached region after full recovery, F0 is the fluorescence intensity just after bleaching (time 0), and Fi is the fluorescence intensity in the prebleach image. F0 values were normalized to 0 in all measurements, and an exponential curve was plotted to the experimental points with the Origin software (OriginLab).

Supplemental Data

The following materials are available in the online version of this article.

Supplemental Figure 1. Comparison of 9-Aminoacridine Quenching, Reflecting Amplitude of ΔpH, in Zea and Vio Chloroplasts upon Light Treatment.

Supplemental Figure 2. Image Analysis Routine for PSII Particles on the EFs Fracture Faces and LHCII Particles on PFs Faces.

Supplemental Table 1. Analysis of EFs Fracture Faces from Electron Micrographs of Wild-Type and PSII Minor Antenna Mutant Intact *Arabidopsis* Chloroplasts.

ACKNOWLEDGMENTS

T.K.G. is supported by a Biotechnology and Biological Sciences Research Council (BBSRC) studentship. The work was supported by BBSRC, Engineering and Physical Sciences Research Council, and Wellcome Trust research and equipment grants to A.V.R. and C.W.M.

Received November 24, 2010; revised March 8, 2011; accepted March 28, 2011; published April 15, 2011.

REFERENCES

Ahn, T.K., Avenson, T.J., Ballottari, M., Cheng, Y.C., Niyogi, K.K., Bassi, R., and Fleming, G.R. (2008). Architecture of a charge-transfer state regulating light harvesting in a plant antenna protein. Science **320:** 794–797.

Andersson, J., Walters, R.G., Horton, P., and Jansson, S. (2001). Antisense inhibition of the photosynthetic antenna proteins CP29 and CP26: implications for the mechanism of protective energy dissipation. Plant Cell **13:** 1193–1204.

Andersson, J., Wentworth, M., Walters, R.G., Howard, C.A., Ruban, A.V., Horton, P., and Jansson, S. (2003). Absence of the Lhcb1 and Lhcb2 proteins of the light-harvesting complex of photosystem II - effects on photosynthesis, grana stacking and fitness. Plant J. **35:** 350–361.

Armond, P.A., Staehelin, L.A., and Arntzen, C.J. (1977). Spatial relationship of photosystem I, photosystem II, and the light-harvesting complex in chloroplast membranes. J. Cell Biol. **73:** 400–418.

Betterle, N., Ballottari, M., Zorzan, S., de Bianchi, S., Cazzaniga, S., Dall'osto, L., Morosinotto, T., and Bassi, R. (2009). Light-induced dissociation of an antenna hetero-oligomer is needed for non-photochemical quenching induction. J. Biol. Chem. **284:** 15255–15266.

Bilger, W., and Björkman, O. (1994). Relationships among violaxanthin deepoxidation, thylakoid membrane conformation, and nonphotochemical chlorophyll fluorescence quenching in leaves of cotton (*Gossypium hirsutum L.*). Planta **193:** 238–246.

Bilger, W., Björkman, O., and Thayer, S.S. (1989). Light-induced spectral absorbance changes in relation to photosynthesis and the epoxidation state of xanthophyll cycle components in cotton leaves. Plant Physiol. **91:** 542–551.

Bode, S., Quentmeier, C.C., Liao, P.N., Hafi, N., Barros, T., Wilk, L., Bittner, F., and Walla, P.J. (2009). On the regulation of photosynthesis by excitonic interactions between carotenoids and chlorophylls. Proc. Natl. Acad. Sci. USA **106:** 12311–12316.

Boekema, E.J., Hankamer, B., Bald, D., Kruip, J., Nield, J., Boonstra, A.F., Barber, J., and Rögner, M. (1995). Supramolecular structure of the photosystem II complex from green plants and cyanobacteria. Proc. Natl. Acad. Sci. USA **92:** 175–179.

Boekema, E.J., van Breemen, J.F.L., van Roon, H., and Dekker, J.P. (2000). Arrangement of photosystem II supercomplexes in crystalline macrodomains within the thylakoid membrane of green plant chloroplasts. J. Mol. Biol. **301:** 1123–1133.

Boekema, E.J., van Roon, H., and Dekker, J.P. (1998). Specific association of photosystem II and light-harvesting complex II in partially solubilized photosystem II membranes. FEBS Lett. **424:** 95–99.

Boekema, E.J., Van Roon, H., Van Breemen, J.F.L., and Dekker, J.P. (1999). Supramolecular organization of photosystem II and its light-harvesting antenna in partially solubilized photosystem II membranes. Eur. J. Biochem. **266:** 444–452.

Bonardi, V., Pesaresi, P., Becker, T., Schleiff, E., Wagner, R., Pfannschmidt, T., Jahns, P., and Leister, D. (2005). Photosystem II core phosphorylation and photosynthetic acclimation require two different protein kinases. Nature **437:** 1179–1182.

Briantais, J.M., Vernotte, C., Picaud, M., and Krause, G.H. (1979). A quantitative study of the slow decline of chlorophyll a fluorescence in isolated chloroplasts. Biochim. Biophys. Acta **548:** 128–138.

Crouchman, S., Ruban, A., and Horton, P. (2006). PsbS enhances nonphotochemical fluorescence quenching in the absence of zeaxanthin. FEBS Lett. **580:** 2053–2058.

Daum, B., Nicastro, D., Austin II, J., McIntosh, J.R., and Kühlbrandt, W. (2010). Arrangement of photosystem II and ATP synthase in chloroplast membranes of spinach and pea. Plant Cell **22:** 1299–1312.

Dekker, J.P., and Boekema, E.J. (2005). Supramolecular organization of thylakoid membrane proteins in green plants. Biochim. Biophys. Acta **1706:** 12–39.

Dekker, J.P., van Roon, H., and Boekema, E.J. (1999). Heptameric association of light-harvesting complex II trimers in partially solubilized photosystem II membranes. FEBS Lett. **449:** 211–214.

Demmig-Adams, B. (1990). Carotenoids and photoprotection: A role for the xanthophyll zeaxanthin. Biochim. Biophys. Acta **1020:** 1–24.

Gilmore, A.M., Hazlett, T.L., and Govindjee. (1995). Xanthophyll cycle-dependent quenching of photosystem II chlorophyll a fluorescence: Formation of a quenching complex with a short fluorescence lifetime. Proc. Natl. Acad. Sci. USA **92:** 2273–2277.

Goral, T.K., Johnson, M.P., Brain, A.P.R., Kirchhoff, H., Ruban, A.V., and Mullineaux, C.W. (2010). Visualizing the mobility and distribution of chlorophyll proteins in higher plant thylakoid membranes:

Effects of photoinhibition and protein phosphorylation. Plant J. **62:** 948–959.

Hager, A. (1969). Lichtbedingte pH-Erniedrigung in einem Chloroplastenkompartiment als Ursache der enzymatischen Violaxanthin- Zeaxanthin-Umwandlung; Bezie-hungen zur Photophosphorylierung. Planta **89:** 224–243.

Hankamer, B., Barber, J., and Boekema, E.J. (1997). Structure and membrane organization of photosystem II in green plants. Annu. Rev. Plant Physiol. Plant Mol. Biol. **48:** 641–671.

Holt, N.E., Zigmantas, D., Valkunas, L., Li, X.P., Niyogi, K.K., and Fleming, G.R. (2005). Carotenoid cation formation and the regulation of photosynthetic light harvesting. Science **307:** 433–436.

Holzwarth, A.R., Miloslavina, Y., Nilkens, M., and Jahns, P. (2009). Identification of two quenching sites active in the regulation of photosynthetic light-harvesting studied by time-resolved fluorescence. Chem. Phys. Lett. **483:** 262–267.

Horton, P., Johnson, M.P., Perez-Bueno, M.L., Kiss, A.Z., and Ruban, A.V. (2008). Photosynthetic acclimation: Does the dynamic structure and macro-organisation of photosystem II in higher plant grana membranes regulate light harvesting states? FEBS J. **275:** 1069–1079.

Horton, P., Ruban, A.V., Rees, D., Pascal, A.A., Noctor, G., and Young, A.J. (1991). Control of the light-harvesting function of chloroplast membranes by aggregation of the LHCII chlorophyll-protein complex. FEBS Lett. **292:** 1–4.

Horton, P., Ruban, A.V., and Walters, R.G. (1996). Regulation of light harvesting in green plants. Annu. Rev. Plant Physiol. Plant Mol. Biol. **47:** 655–684.

Horton, P., Wentworth, M., and Ruban, A. (2005). Control of the light harvesting function of chloroplast membranes: The LHCII-aggregation model for non-photochemical quenching. FEBS Lett. **579:** 4201–4206.

Ilioaia, C., Johnson, M.P., Duffy, C.D.P., Pascal, A.A., van Grondelle, R., Robert, B., and Ruban, A.V. (2011). Origin of absorption changes associated with photoprotective energy dissipation in the absence of zeaxanthin. J. Biol. Chem. **286:** 91–98.

Iwai, M., Yokono, M., Inada, N., and Minagawa, J. (2010). Live-cell imaging of photosystem II antenna dissociation during state transitions. Proc. Natl. Acad. Sci. USA **107:** 2337–2342.

Johnson, M.P., Havaux, M., Triantaphylidès, C., Ksas, B., Pascal, A. A., Robert, B., Davison, P.A., Ruban, A.V., and Horton, P. (2007). Elevated zeaxanthin bound to oligomeric LHCII enhances the resistance of Arabidopsis to photooxidative stress by a lipid-protective, antioxidant mechanism. J. Biol. Chem. **282:** 22605–22618.

Johnson, M.P., Pérez-Bueno, M.L., Zia, A., Horton, P., and Ruban, A.V. (2009). The zeaxanthin-independent and zeaxanthin-dependent qE components of nonphotochemical quenching involve common conformational changes within the photosystem II antenna in *Arabidopsis.* Plant Physiol. **149:** 1061–1075.

Johnson, M.P., and Ruban, A.V. (2009). Photoprotective energy dissipation in higher plants involves alteration of the excited state energy of the emitting chlorophyll(s) in the light harvesting antenna II (LHCII). J. Biol. Chem. **284:** 23592–23601.

Kereïche, S., Kiss, A.Z., Kouril, R., Boekema, E., and Horton, P. (2010). The PsbS protein controls the macro-organisation of photosystem II complexes in the grana membarnes of higher plant chloroplasts. FEBS Lett. **584:** 754–764.

Kirchhoff, H., Haase, W., Haferkamp, S., Schott, T., Borinski, M., Kubitscheck, U., and Rögner, M. (2007b). Structural and functional self-organization of Photosystem II in grana thylakoids. Biochim. Biophys. Acta **1767:** 1180–1188.

Kirchhoff, H., Haase, W., Wegner, S., Danielsson, R., Ackermann, R., and Albertsson, P.A. (2007a). Low-light-induced formation of semicrystalline photosystem II arrays in higher plant chloroplasts. Biochemistry **46:** 11169–11176.

Kirchhoff, H., Haferkamp, S., Allen, J.F., Epstein, D.B.A., and Mullineaux, C.W. (2008). Protein diffusion and macromolecular crowding in thylakoid membranes. Plant Physiol. **146:** 1571–1578.

Kiss, A.Z., Ruban, A.V., and Horton, P. (2008). The PsbS protein controls the organization of the photosystem II antenna in higher plant thylakoid membranes. J. Biol. Chem. **283:** 3972–3978.

Kovács, L., Damkjaer, J., Kereïche, S., Ilioaia, C., Ruban, A.V., Boekema, E.J., Jansson, S., and Horton, P. (2006). Lack of the light-harvesting complex CP24 affects the structure and function of the grana membranes of higher plant chloroplasts. Plant Cell **18:** 3106–3120.

Li, X.P., Björkman, O., Shih, C., Grossman, A.R., Rosenquist, M., Jansson, S., and Niyogi, K.K. (2000). A pigment-binding protein essential for regulation of photosynthetic light harvesting. Nature **403:** 391–395.

Li, X.P., Gilmore, A.M., Caffarri, S., Bassi, R., Golan, T., Kramer, D., and Niyogi, K.K. (2004). Regulation of photosynthetic light harvesting involves intrathylakoid lumen pH sensing by the PsbS protein. J. Biol. Chem. **279:** 22866–22874.

Liao, P.N., Bode, S., Wilk, L., Hafi, N., and Walla, P.J. (2010). Correlation of electronic carotenoid–chlorophyll interactions and fluorescence quenching with the aggregation of native LHCII and chlorophyll deficient mutants. Chem. Phys. **373:** 50–55.

Liu, Z.F., Yan, H.C., Wang, K.B., Kuang, T.Y., Zhang, J.P., Gui, L.L., An, X.M., and Chang, W.R. (2004). Crystal structure of spinach major light-harvesting complex at 2.72 A resolution. Nature **428:** 287–292.

Lokstein, H., Tian, L., Polle, J.E.W., and DellaPenna, D. (2002). Xanthophyll biosynthetic mutants of *Arabidopsis thaliana*: Altered nonphotochemical quenching of chlorophyll fluorescence is due to changes in photosystem II antenna size and stability. Biochim. Biophys. Acta **1553:** 309–319.

Ma, Y.Z., Holt, N.E., Li, X.P., Niyogi, K.K., and Fleming, G.R. (2003). Evidence for direct carotenoid involvement in the regulation of photosynthetic light harvesting. Proc. Natl. Acad. Sci. USA **100:** 4377–4382.

Miller, K.R., Miller, G.J., and McIntyre, K.R. (1976). The light-harvesting chlorpohyll-protein complex of photosystem II. Its location in the photosynthetic membrane. J. Cell Biol. **71:** 624–638.

Miloslavina, Y., Wehner, A., Lambrev, P.H., Wientjes, E., Reus, M., Garab, G., Croce, R., and Holzwarth, A.R. (2008). Far-red fluorescence: a direct spectroscopic marker for LHCII oligomer formation in non-photochemical quenching. FEBS Lett. **582:** 3625–3631.

Müller, M.G., Lambrev, P., Reus, M., Wientjes, E., Croce, R., and Holzwarth, A.R. (2010). Singlet energy dissipation in the photosystem II light-harvesting complex does not involve energy transfer to carotenoids. ChemPhysChem **11:** 1289–1296.

Murakami, S., and Packer, L. (1970a). Light-induced changes in the conformation and configuration of the thylakoid membrane of *Ulva* and *Porphyra* chloroplasts *in vivo.* Plant Physiol. **45:** 289–299.

Murakami, S., and Packer, L. (1970b). Protonation and chloroplast membrane structure. J. Cell Biol. **47:** 332–351.

Peter, G.F., and Thornber, J.P. (1991a). Biochemical evidence that the higher-plant photosystem II core complex is organized as a dimer. Plant Cell Physiol. **32:** 1237–1250.

Peter, G.F., and Thornber, J.P. (1991b). Biochemical composition and organization of higher plant photosystem II light-harvesting pigment-proteins. J. Biol. Chem. **266:** 16745–16754.

Porra, R.J., Thompson, W.A., and Kriedemann, P.E. (1989). Determination of accurate extinction coefficients and simultaneous equations for assaying chlorophyll *a* and chlorophyll *b* extracted with 4 different

solvents: Verification of the concentration of chlorophyll standards by atomic absorption spectroscopy. Biochim. Biophys. Acta **975:** 384–394.

Powles, S.B. (1984). Photoinhibition of photosynthesis induced by visible-light. Annu. Rev. Plant Physiol. Plant Mol. Biol. **35:** 15–44.

Ruban, A.V., Berera, R., Ilioaia, C., van Stokkum, I.H., Kennis, J.T., Pascal, A.A., van Amerongen, H., Robert, B., Horton, P., and van Grondelle, R. (2007). Identification of a mechanism of photoprotective energy dissipation in higher plants. Nature **450:** 575–578.

Ruban, A.V., Calkoen, F., Kwa, S.L.S., van Grondelle, R., Horton, P., and Dekker, J.P. (1997). Characterisation of LHCII in the aggregated state by linear and circular dichroism spectroscopy. Biochim. Biophys. Acta **1321:** 61–70.

Ruban, A.V., and Horton, P. (1999). The xanthophyll cycle modulates the kinetics of non-photochemical energy dissipation in isolated light-harvesting complexes, intact chloroplasts and leaves of spinach. Plant Physiol. **119:** 531–542.

Ruban, A.V., Lee, P.J., Wentworth, M., Young, A.J., and Horton, P. (1999). Determination of the stoichiometry and strength of binding of xanthophylls to the photosystem II light harvesting complexes. J. Biol. Chem. **274:** 10458–10465.

Ruban, A.V., Pascal, A.A., Robert, B., and Horton, P. (2002). Activation of zeaxanthin is an obligatory event in the regulation of photosynthetic light harvesting. J. Biol. Chem. **277:** 7785–7789.

Ruban, A.V., Rees, D., Noctor, G.D., Young, A.J., and Horton, P. (1991). Long wavelength chlorophyll species are associated with amplification of high energy state quenching in higher plants. Biochim. Biophys. Acta **1059:** 355–360.

Ruban, A.V., Rees, D., Pascal, A.A., and Horton, P. (1992). Mechanism of ΔpH-dependent dissipation of absorbed excitation energy by photosynthetic membranes. 2. The relationship between LHCII aggregation *in vitro* and qE in isolated thylakoids. Biochim. Biophys. Acta **1102:** 39–44.

Ruban, A.V., Young, A.J., and Horton, P. (1993). Induction of non-photochemical quenching and absorbance changes in leaves. Plant Physiol. **102:** 741–750.

Simpson, D.J. (1979). Freeze-fracture studies on barley plastid membranes. III. Location of the light harvesting chlorophyll-protein. Carlsberg Res. Commun. **44:** 305–336.

Simpson, D.J. (1982). Freeze-fracture studies on barley plastid membranes *V. viridis*-n34, a photosystem I mutant. Carlsberg Res. Commun. **47:** 215–225.

Staehelin, L.A. (1976). Reversible particle movements associated with unstacking and restacking of chloroplast membranes *in vitro.* J. Cell Biol. **71:** 136–158.

Staehelin, L.A. (2003). Chloroplast structure: from chlorophyll granules to supra-molecular architecture of thylakoid membranes. Photosynth. Res. **76:** 185–196.

Walters, R.G., Ruban, A.V., and Horton, P. (1994). Higher plant light-harvesting complexes LHCIIa and LHCIIc are bound by dicyclohexylcarbodiimide during inhibition of energy dissipation. Eur. J. Biochem. **226:** 1063–1069.

Wraight, C.A., and Crofts, A.R. (1970). Energy-dependent quenching of chlorophyll alpha fluorescence in isolated chloroplasts. Eur. J. Biochem. **17:** 319–327.

Yamamoto, H.Y., Nakayama, T.O., and Chichester, C.O. (1962). Studies on the light and dark interconversions of leaf xanthophylls. Arch. Biochem. Biophys. **97:** 168–173.